Int. J. Electrochem. Sci., 7 **(2012)** 12034 - 12044

International Journal of
ELECTROCHEMICAL
SCIENCE
www.electrochemsci.org

Electrodeposition of Macroporous Zn and ZnO Films from Ionic Liquids

Nguyet Doan, Tuomas Vainikka, Eeva-Leena Rautama, Kyösti Kontturi, Christoffer Johans[*]

Department of Chemistry, School of Chemical Technology, Aalto University, PO Box 16100, 00076 Aalto, Finland
[*]E-mail: christoffer.johans@aalto.fi

Received: 2 October 2012 / *Accepted:* 3 November 2012 / *Published:* 1 December 2012

Nanostructured zinc films were prepared by electrodeposition onto templates of well-ordered regular arrays of PS spheres on ITO and gold coated glass substrates. The deposition was carried out from an ionic liquid (1-butyl-1-methylpyrrolidinium bis(trifluoromethanesulfonyl)imide) at room temperature in an argon filled glove box. The Zn films were oxidized to ZnO when exposed to air at elevated temperature. SEM images showed well organized nanostructures for both Zn and ZnO.

Keywords: zinc, zinc oxide, ionic liquids, polystyrene templates, electrodeposition

1. INTRODUCTION

Zinc oxide (ZnO) is a semiconductor with a direct band gap of 3.37 eV (375 nm) with a relatively large excitation binding energy of 60 meV. These properties make it a promising material for optoelectronic applications, e.g. light emitting diodes (LEDs) [1-5]. While n-doping is easy to achieve, reliable p-doping remains difficult. To overcome the limitations imposed by the lack of p-doping, n-type ZnO has been combined with other materials such as p-type GaN. ZnO has also been used as a transparent current spreading layer on GaN LEDs [6]. Our interest is in textured ZnO films, which can favorably out couple light from the LED chip by reducing total internal reflection through increased surface roughness and diffraction from periodic structures.

Deposition onto self-assembled colloidal crystals is a useful method for producing such structured arrays on surfaces and the technique has attracted much attention in the last few years due to the numerous potential applications in biomedical sciences, electronics, optics, energy storage and electrochemistry [7-9]. The length scale of the features is typically of the same order of magnitude as light, and can be well controlled by the size of the colloidal particles.

Electrodeposition of macroporous zinc oxide onto templates has been widely researched. However, it is still not easy to obtain qualitatively good films. Most of the work has been performed with nitrate ions as the oxygen precursor. Commonly, electrodeposition has been performed from a 0.04-0.1 M zinc nitrate bath maintained at temperatures between 62-80 °C. [10-13] Ramirez and *et. al.*[14] used hydrogen peroxide as an oxygen precursor to prepare macroporous zinc oxide films. It was shown that at low H_2O_2 concentration large ZnO grains were formed, which did not fill the template densely, while at higher concentration, the template was densely filled with nanocrystalline ZnO [14]. While there are many publications dealing with ZnO electrodeposition onto templates, electrodeposition of metallic zinc have been less studied [15]. The deposition of Zinc from aqueous solutions requires negative potentials E^0=-0.76 V vs SHE and acidic conditions, and is only possible due to the high overpotential of hydrogen reduction at the zinc surface.

Ionic liquids (ILs) have become an increased field of interest because of their unique properties and potential applications [16-18]. They are also attractive for electrodeposition of reactive metals due to the large potential window. The ILs also offer solvation environments that are different from water, and provide altered nucleation rates and growth mechanisms. Yavari *et al.* [19] studied the morphology of ZnO prepared by a hydrothermal route in different ILs as morphology templates. The morphology of the ZnO changes from rod-like to star-like and flower-like in different ILs. Recently, Azaceta *et al.* [20] studied the influence of the Zn^{2+} concentration and temperature on the electrochemical reduction of O_2 in a solution of zinc bis(trifluoromethanesulfonyl)imide ($Zn(TFSI)_2$) salt in 1-butyl-1-methylpyrrolidinium bis(trifluoromethanesulfonyl)imide (PYR14TFSI) ionic liquid. ZnO nanocrystalline films were then electrodeposited, under enhanced O_2 reduction, at temperatures in the 75–150°C range. The morphologies, chemical composition, structural and optical properties of ZnO films were analysed.

In this paper, we prepare ZnO films by electrodepositing metallic Zn onto colloidal crystal templates, then removing the template, and finally oxidizing the film in air at elevated temperatures. Well-ordered nanostructured films of Zn were deposited onto regular arrays of 600 nm spherical polystyrene spheres on gold and ITO substrates. The thickness of the film was optimized by changing the deposition charge. The templates on the ITO and Au- substrates and the structured Zn films were characterized using scanning electron microscopy (SEM JSM-7500F) coupled with energy-dispersive X-ray spectroscopy (EDS) and X-ray diffraction (XRD).

2. EXPERIMENTAL

The substrates used were indium titanium oxide coated glass (ITO, Planar Systems Oy, Finland) and gold coated glass (Platypus, 500 Å of gold over a 25 Å a titanium adhesion layer). The substrates were cleaned in acetone (99.5%, Merck) for 1 hour and in ethanol (Etax, 99.6 %, Altia) for 1 hour and then dried under a nitrogen stream. The polystyrene sphere templates were prepared as described previously [21]. Briefly, a small void for the polystyrene sphere solution was created by separating the substrate from a glass slide using one layer of parafilm (Pechiney Plastic Inc.) as a spacer. The template area was 1.0 x1.5 cm^2. The void was filled with polystyrene sphere (PS) colloid (600 nm, Thermo Scientific, 1% solids by weight) using a 1 μl micro-pipette, and the sample was

placed into a refrigerator (Cuisinart, Hobby hall, Finland) cooled by a Peltier element at a constant temperature of 13 °C. The template was tilted with an inclination of 15° from the horizontal plane for about 40 hours. After the water had evaporated, the electrode area was limited by masking the template free area with nail varnish (Malava, colourless).

The Zinc salt used in the electroplating solution was prepared by adding an excess of Zinc Oxide (p.a., Riedel-de Haën) to an aqueous solution of bis(trifluoromethylsulfonyl)imide (99 %, Acros Organics). The mixture was filtered to remove the excess ZnO, and then the water was removed with a nitrogen purge followed by an overnight vacuum treatment in a vacuum oven before the salt was transferred inside an Argon filled glove box (<2 ppm H_2O, <2 ppm O_2, Vacuum Atmospheres Company). The resulting salt Zinc di(bis(trifluorometylsulfonyl)imide), $Zn(TFSI)_2$ had a purity of 93.3% (Zn basis) analyzed using flame AAS (Perkin Elmer). This indicates a slight excess of bis(trifluoromethylsulfonyl)imide. The electroplating solution was a mixture of 1-butyl-1-methylpyrrolidinium bis(trifluoromethylsulfonyl)imide, $PYR_{14}TFSI$ (98.5%, Fluka) and the synthesized $Zn(TFSI)_2$.

The Zn structures were deposited in the glove box from an electroplating solution containing 49 mM $Zn(TFSI)_2$. Electrochemical experiments were carried out using a PAR263A potentiostat controlled with in-house developed software. A three electrode setup with a zinc spiral as a counter electrode and a zinc wire as a reference electrode was used for the electrochemical characterization. A two-electrode setup with a Zinc spiral as a combined counter and reference electrode was used for the deposition experiments. The templated ITO and Au substrates were used as working electrodes. Before the deposition onto the PS template substrates, bare ITO and Au substrates were analysed using cyclic voltammetry to determine the deposition behaviour and potentials. The temperature inside the glove box was approximately 25 °C. Zn structures were deposited on the ITO substrate at a constant potential of -1.6 V vs. Zn/Zn^{2+}, and on the Au substrate with -1.65 V vs. Zn/Zn^{2+}. The film thickness was optimised with the deposition charge. Charge densities of -0.095 C/cm^2 gave a thickness approximately equal to half the PS sphere, which was suitable for the purpose of this study.

After deposition, the substrates were taken out from the glove box and the PS templates were removed by immersing the samples in N,N-dimethylformamide (DMF, Fisher Scientific, 99.96%) for 45 min. The samples were analysed. Then, samples were heated in an oven at 400 °C for 20 hours. Before heating, the colours of the deposited samples were black-grey and after heating the colour changed to white, which indicated that Zn had been oxidized to ZnO.

Polystyrene sphere templates and the Zn and ZnO films were characterized by scanning electron microscopy (SEM JSM-7500F) coupled with energy-dispersive X-ray spectroscopy (EDS). The crystallinity of the Zn and ZnO was studied by X-ray diffraction (XRD; PanAnalytical X'pert Pro MPD, Cu $K\alpha_1$ radiation). The samples were attached to a zero sample holder and the data was corrected for their angular shift.

3. RESULTS AND DISCUSSIONS

Cyclic voltammograms of bare gold and ITO substrates in $PYR_{14}TFSI$ with 49 mM $Zn(TFSI)_2$ are shown in Figure 1. The voltammograms show typical features of a deposition process, with Zinc

(see later for analysis) deposited when the potential is swept in the negative direction starting around -0.7 V vs Zn/Zn^{2+}. The corresponding dissolution peak is observed at approximately 0.3 V vs Zn/Zn^{2+}, with the increase of the current starting already from 0 V vs. Zn/Zn^{2+} when sweeping in the positive direction, as expected. The deposited and stripped charges agree well, indicating that current efficiency for the deposition process is high and that all deposited material adheres to the electrode for both the gold and ITO substrates. The differences between the voltammograms recorded at gold and ITO were subtle and varied slightly with time. Typically the deposition on gold was shifted by 50 mV in the negative direction. Azaceta *et al.*[20] have studied the deposition of ZnO from the same IL electrolyte system at temperatures in the 50-150°C range. Our cyclic voltammograms agree well with the cyclic voltammogram for zinc deposition on fluorine doped tin oxide shown in their supplementary information, however, the overpotential observed here is significantly larger, which can primarily be attributed to the lower temperature used in our study and the difference between the substrates. It should also be noted that our experiments were performed under a nitrogen atmosphere in a dry box. Thus, contamination by water or oxygen that may aid in the nucleation process is therefore unlikely.

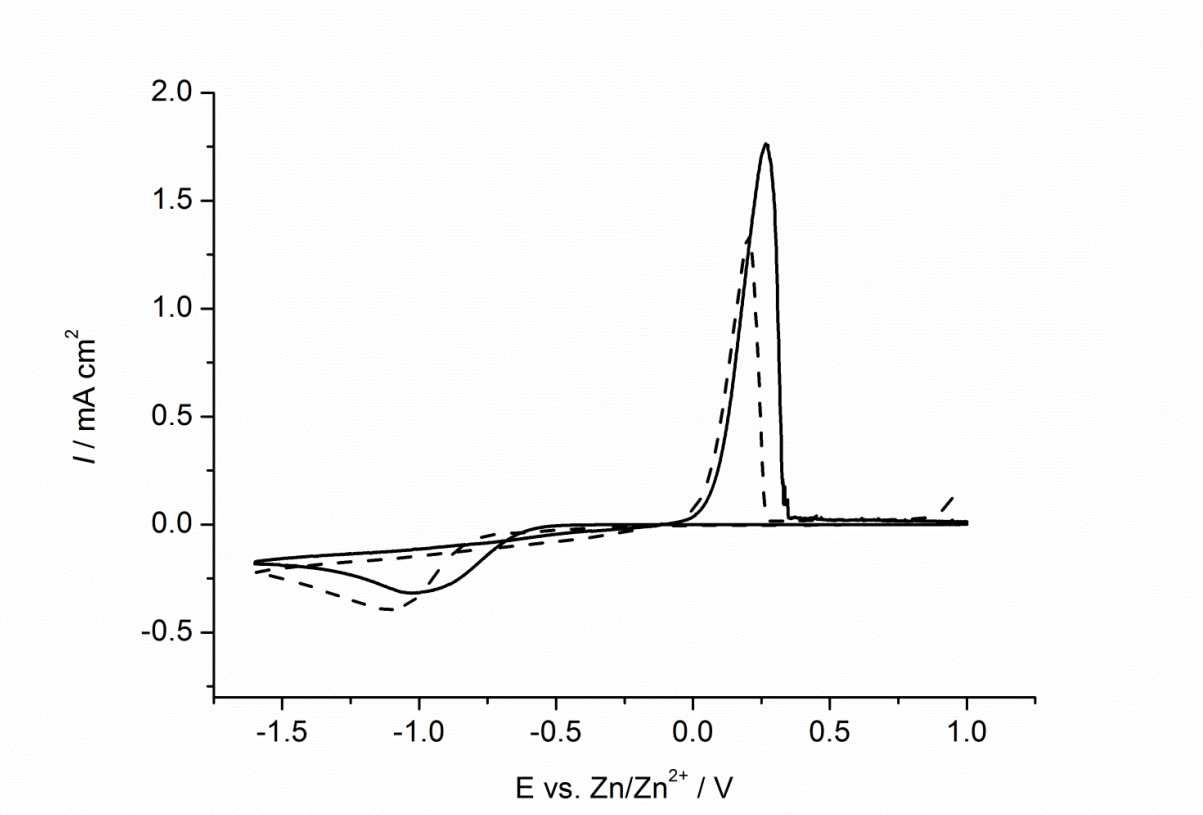

Figure 1. Cyclic voltammograms of (solid line) ITO and (dashed line) gold electrodes in 49 mM $Zn(TFSI)_2$ in $PYR_{14}TFSI$. The sweep rate was 0.01 V/s. A peak corresponding to deposition of metallic Zinc is observed at approx. -1.0 V and the corresponding stripping peak at approx. 0.3 V. The experiments were performed at 25°C in a glove box.

SEM images of the PS templates can be seen in Figure 2 for the gold and ITO substrates. The bright coloured areas are due to charging artefacts of the non-conducting PS spheres in the electron beam, and do not reflect different composition, morphology or ordering of the templates. The quality

of the template is crucial to obtain optimal films [14], since the local order affects the current distribution and subsequently film deposition. A well organized, uniform monolayer of PS spheres can be observed. No areas of multilayers could be observed on the electrode area, however, point defects constituted of vacancies are observed, see Figure 2.

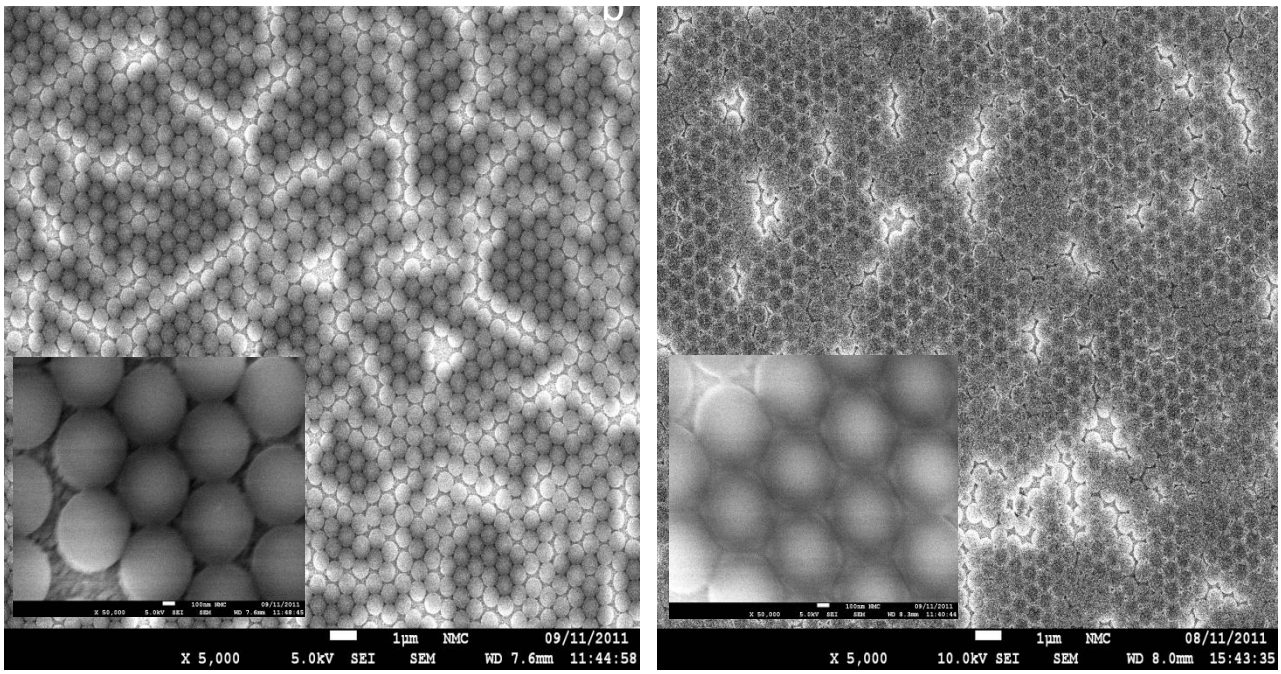

Figure 2. SEM images of 600 nm PS template on a) ITO and b) on Au- substrates.

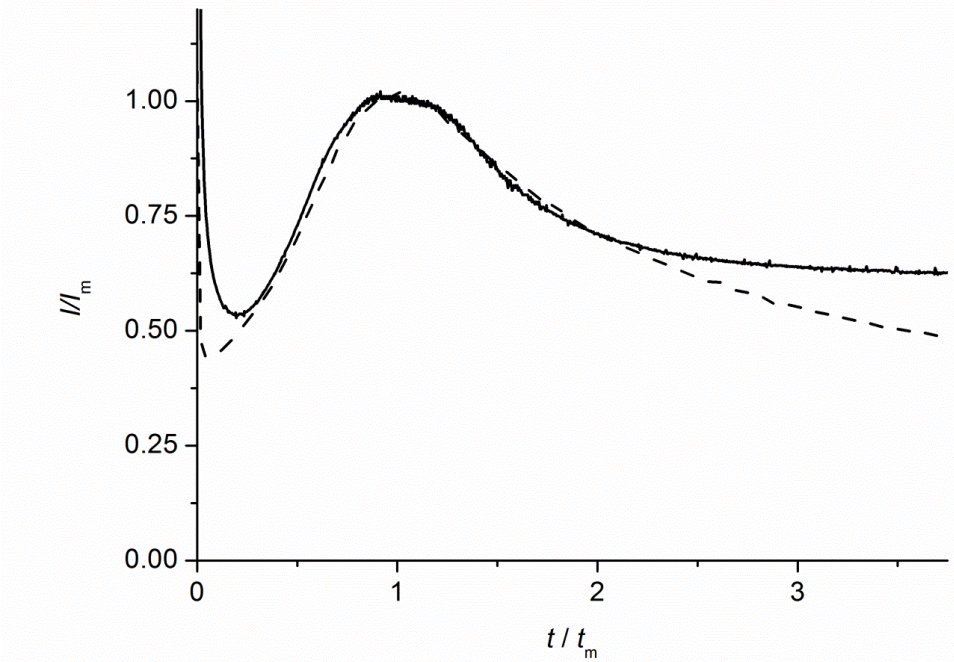

Figure 3. The current transients reduced by peak current and time obtained for electrodepostion Zn through a 600 nm sphere template on (solid line) ITO and (dashed line) Au coated substrate at -1.6 and -1.65 V in 49 mM ($Zn(TFSI)_2$) in the ($PYR_{14}TFSI$) based electrolytes at 25 °C. The experiment was performed in the glove box.

Due to limitations on cell design the deposition experiments were carried out in two electrode mode with a zinc spiral as a counter electrode. The two electrode setup has several drawbacks compared to the three-electrode setup, particularly the high iR-drop in the electrolyte solution due to uncompensated solution resistance. The combined zinc counter and reference electrode works satisfactorily in the deposition experiments since already small polarization of the counter/reference electrode in the positive direction leads to large currents resulting from the dissolution of Zinc ions from the wire, however, care has to be taken when relating the deposition voltage to the voltammograms. Several voltages were tested and the best deposits were obtained with -1.65 V and -1.6 V for the gold and ITO substrates, respectively. At lower voltages no zinc deposits were observed at the electrode surface or the adhesion was poor. This trend was independent of the electrode substrate.

The experimentally determined optimal deposition potentials were higher than the peak currents in the cyclic voltammograms. This is attributed to the uncompensated solution resistance, which in ionic liquids [22] easily reaches a few hundred millivolts. Higher deposition potentials resulted in uneven films, while at lower potentials the coverage was incomplete The current-time transients for electrodeposition of Zn onto 600 nm PS sphere templates on gold and ITO substrates are shown in Figure 3 in reduced format. Typical features of nucleation can be seen, i.e. after the initial capacitive charging peak, the magnitude of the current slowly increases corresponding to nucleation and growth of a new phase at the electrode surface, followed by a slow decrease in current due to the development of a linear diffusion regime [23]. While this type of phenomena has been widely studied and modelled at bulk solution-electrode interfaces, the mass transfer in the polystyrene matrix must be accounted for, before quantitative models can be applied here.

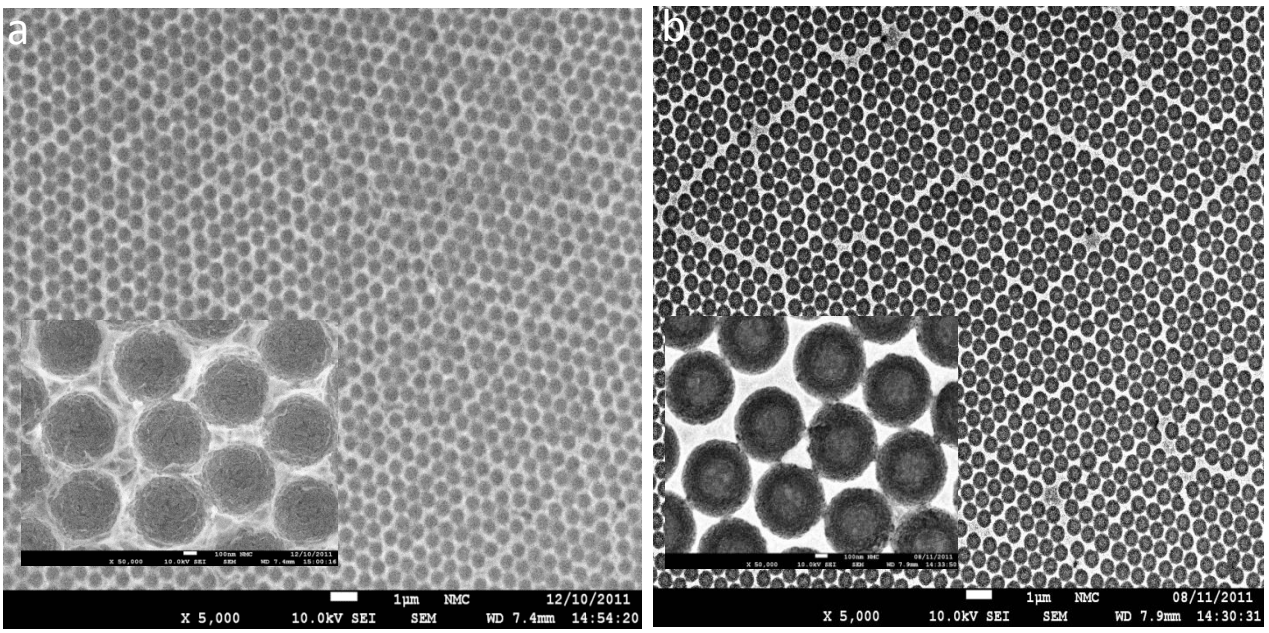

Figure 4. SEM images of Zn nanostructured films from 49 mM ($Zn(TFSI)_2$) in ($PYR_{14}TFSI$) ionic liquids at 25 °C, on a) on ITO and b) on Au-substrates after the PS beads were dissolved in DMF.

SEM images of the deposited zinc structures after removal of the PS template are shown in Figure 4. The white areas correspond to deposited zinc and the dark areas to the voids left by the PS spheres. The insets in the figure show the structure at higher magnification. In addition to the electrodeposition parameters, such as potential, deposition time and temperature the structure of the substrate affects the morphology of the deposited films [24, 25]. The Zn films obtained on gold were more even than on ITO. The difference observed here probably follows from the favourable lattice match between zinc and gold, compared to the rather large structural difference between zinc and ITO. The ITO films used here were crystalline, as evident from the XRD analysis shown in the Supplementary information.

The thickness of the film can be estimated from the width of the ridge between the holes using simple geometric considerations when the bead size is known. Here, we attempted to limit the thickness of the film to equal the radius of the PS spheres. This was obtained with a charge density of -0.095 C/cm^2 on both substrates. As can be observed, the width of the ridge is very narrow on both substrates, and hence the film is approximately 300 nm thick. The theoretical deposition charge required to obtain 300 nm a dense film onto the template is -0.330 C/cm^2. Comparison to the experimentally observed value indicates that the film is rather porous.

Energy dispersive X-ray spectroscopy (EDS, Supplementary information) show the presence of zinc on both gold and ITO. Both samples have oxygen present in significant amounts, which is expected since the samples have been exposed to air prior to analysis. The resolution of the technique does not allow for conclusions regarding the extent of oxidation.

XRD analyses were also made for the samples. Prior to oxidation at elevated temperatures the deposited film was grey, and the XRD analysis, see Supplementary information, revealed three additional reflections compared to a pure ITO glass measured for background.

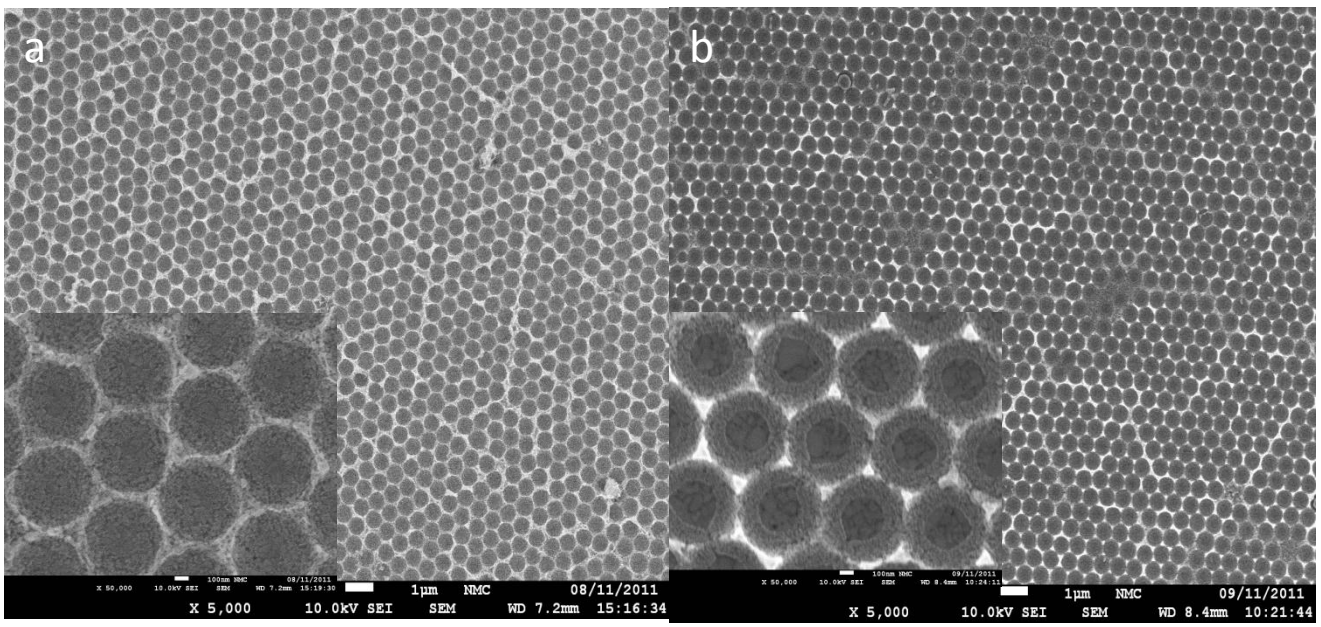

Figure 5. SEM images of Zn nanostructured films from 49 mM ($Zn(TFSI)_2$) in ($PYR_{14}TFSI$) ionic liquids at 25 °C, on a) on ITO and b) on Au-substrates after PS have dissolved out in DMF and heating at 400 °C for 20 hours.

These Bragg peaks account for the 101, 002 and 100 reflections, i.e. the most intensive ones, of hexagonal metallic zinc (reference card # 04-014-0235).

When the samples were heated in an oven at 400 °C for 20 hours, the color of the deposited samples changed from black-grey to white, which indicated that the Zn had been oxidized to ZnO. The SEM images and XRD analysis of the oxidized samples are shown in Figures 5 and 6. The SEM image shows that the heating process did not damage the structure of the film. We believe that the porous nature of the film allows for the 60 % increase in molar volume between Zn and ZnO. The XRD patterns were measured for the plain ITO substrate, and for the oxidized samples on ITO and Au(111) surfaces. The Bragg reflections originating from the ZnO phase were detectable, while metallic Zn could no longer be observed after the oxidation. The patterns were compared to bulk ZnO. Figure 6 presents the experimental XRD patterns and a simulated pattern of hexagonal ZnO (*P*6$_3$*mc*, *a* = 3.2533 Å, *c* = 5.2073 Å**)** for reference. The additional reflections of the ZnO-ITO sample are easily identified as ZnO whereas some discrepancy is observed in the case of the ZnO-Au(111) sample; the 002 and 101 reflections are somewhat shifted with respect to the reference zincite and ZnO-ITO material (note that we have corrected the experimental shift due to sample holder preparation).

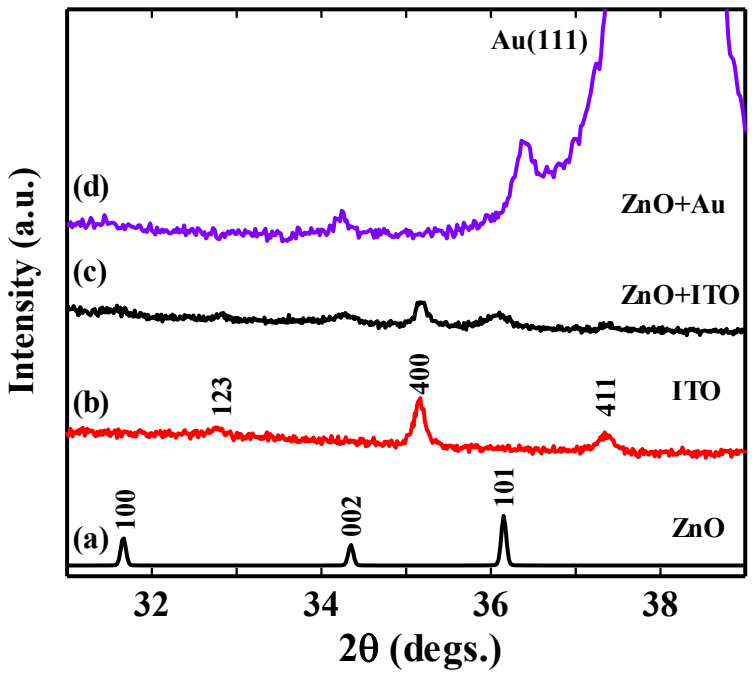

Figure 6. XRD patterns of (a) calculated bulk ZnO (*P*6$_3$*mc*, *a* = 3.253 Å, *c* = 5.207 Å), (b) ITO substrate (*Ia*-3, *a* ≈ 10,2 Å), (c) ZnO deposited on ITO substrate and (d) ZnO deposited on Au(111) substrate. The Miller indices are presented to aid the identification.

There are a few possible explanations for this phenomenon: either it is caused by the strains in the films that are known to shift the Bragg peak positions or the fact that non-stoichiometry introduced by cation vacancies (i.e. $Zn_{1+x}O$) is present in the sample which inevitably affects the lattice parameters

(see e.g. refs. [26, 27]). In fact, there are several reference patterns in the ICDD database for ZnO whose *c* axes differ even by 0.5 %, possibly due to the non-stoichiometry effect on the crystal lattice. Depending on which one is chosen, the reflections can be explained.

4. CONCLUSIONS

We have shown here that regularly structured films of Zn metal and ZnO can be deposited onto gold and ITO substrates templated with polystyrene beads. The depositions were carried out with 1-butyl-1-methylpyrrolidinium bis(trifluoromethylsulfonyl)imide based ionic liquid at room temperature in an argon filled glove box. Deposition of metallic zinc films onto polystyrene bead templates in a ionic liquid media have not been reported previously. Subsequent oxidation of the films at elevated temperature yielded structured ZnO films. The results of this work showed that high quality template Zn and ZnO films can be electrodeposited from ionic liquid onto both semiconductor and metallic substrates.

ACKNOWLEDGMENTS
The authors would like to thank the MIDE for financial support (N.D., C.J.), prof. Bartlett, Dr. J. Sinha from Southampton University for teaching how to prepare templates (N.D.) and Hannu Revitzer for the AAS analysis.

References

1. A. Bakin, A. Behrends, A. Waag, H-J. Lugauer, A. Laubsch, K. Streubel IEEE Proceedings of the IEEE 98 (2010) 1281
2. L. Schmidt-Mende and J.L. MacManus-Driscoll, *Materials Today* 10 (2007) 40
3. R. Könenkamp, R.C. Word and M. Godinez. *Nano Lett.* 5 (2005) 2005
4. H. Sun, Q.F. Zhang and J.L. Wu. *Nanotechnology* 17 (2006) 2271
5. M. Willander, O. Nur, Q. X. Zhao, L. L. Yang, M. Lorenz, B. Q. Cao, J. Z.Pérez, C. Czekalla, G. Zimmermann, M. Grundmann, A. Bakin, A. Behrends, M. Al-Suleiman, A. El-Shaer, A. Che Mofor, B. Postels, A. Waag, N. Boukos, A. Travlos, H. S. Kwack, J. Guinard and D. Le Si Dang, *Nanotechnology* 20 (2009) 332001
6. C. Bayram, F. H. Teherani, D. J. Rogers, M. Razeghi, *Appl. Phys. Lett*. 93 (2008) 081111
7. Philip N. Bartlett, *The Electrochemical Society Interface*, (2004), 28
8. Philip N. Bartlett, Peter R. Birkin and Mohamed A. Ghanem, *Chem. Commun.* (2000) 1671
9. N. Pérez, A. Hüls, D. Puente, W. González-Vĩnas, E. Castãno, S.M. Olaizola, *Sensors and Actuators B* 126 (2007) 86
10. T. Sumida, Y. Wada, T. Kitamura, and S. Yanagida, *Chem. Lett*. (2001) 38
11. L. Teh, K. Yeo, and C. Wong, *Appl. Phys. Lett.* 89 (2006) 051105.
12. H.Yan, Y. Yang, Z. Fu, B. Yang, Z. Wang, L. Xia, S. Yu, S. Fu,and F. Li, *Chem. Lett.* 34 (2005) 976
13. Z. Liu, Z. Jin, J. Qiu, X.Liu, W.Wu and W. Li, *Semicond. Sci. Technol.* 21 (2006) 60
14. D. Ramirez, P. Bartlett, M.Abdelsalam, H. Gomez, and D. Lincot, *Phys. Stat. Sol.* 205 (2008) 2365
15. B.H.Juarez and C.Lopez, *J.Phys.Chem. B.* 108 (2004) 16708
16. N.V. Plechkovaa and K. R. Seddon, *Chem. Soc. Rev*. 37 (2008) 123

17. T. Welton. *Chem. Rev.* 99 (1999) 2071
18. M.Armand, F. Endres, D. R. MacFarlane, H. Ohno, and B. Scrosati, *Nat. Mater.* 8 (2009) 621
19. I.Yavari, A. R. Mahjoub, E. Kowsari, M.Movahedi, *J. Nanopart. Res.* 11 (2009) 861
20. E. Azaceta, R. Marcilla, D. Mecerreyes, M. Ungureanu, A. Dev, T. Voss, S. Fantini, H.-J.Grande, G.Gabañeroa and R. Tena-Zaera, *Phys. Chem. Chem. Phys*. 13 (2011) 13433
21. R. P. Johnson, J. A. Richardson, T. Brown, P. N. Bartlett, Langmuir 28 (2012) 5464
22. Y. Pan, L. E. Boyd, J. F. Kruplak, W. E. Cleland, Jr., J. S. Wilkes, Charles L. Hussey, *J. Electrochem. Soc.* 158 (2011) F1
23. B. Scharifker, G. Hills, *Electrochim. Acta* 28 (1983) 879
24. B.Cao, F.Sun, W.Cai, *Electrochemical and Solid-State Lett*. 8 (2005), G237
25. M. Tulodziecki, J.-M.Tarascon, P.L. Taberna and C.Guery, *J.Electrochem. Soc*. 152 (2012) D691
26. M.J. Brett, R.R. Parsons, *J. Mater. Sci*. 22 (1987) 3611
27. J. Malm, E. Sahramo, J. Perala, T. Sajavaara, M. Karppinen, *Thin Solid Films* 519 (2011) 5319

Supplementary information:

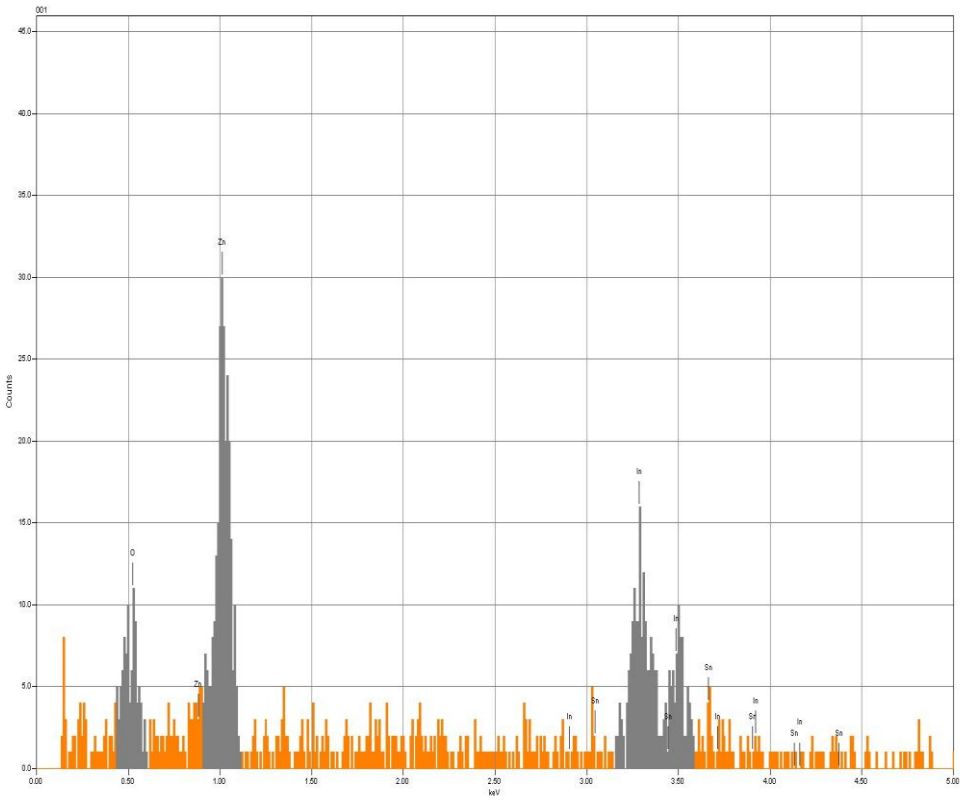

Figure s1. Energy dispersive X-ray spectroscopy spectrum shows the presence of zinc on ITO substrate.

ZnO films were characterized by scanning electron microscopy (SEM JSM-7500F) coupled with energy-dispersive X-ray spectroscopy (EDS). The samples were placed onto the sample holder by using carbon tape.

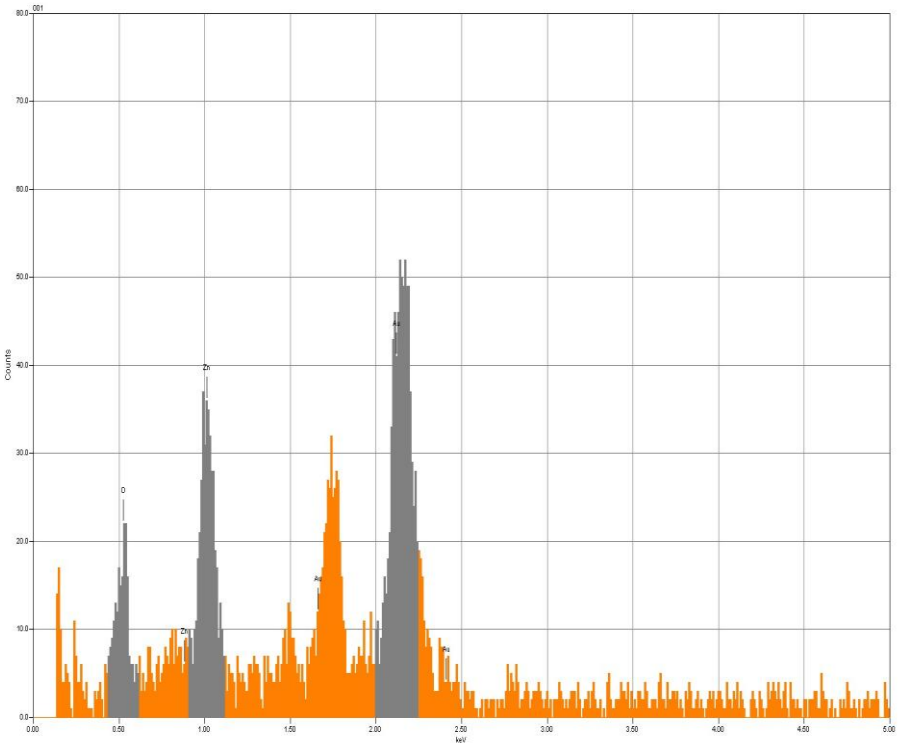

Figure s2. Energy dispersive X-ray spectroscopy spectrum shows the presence of zinc on Au substrate.

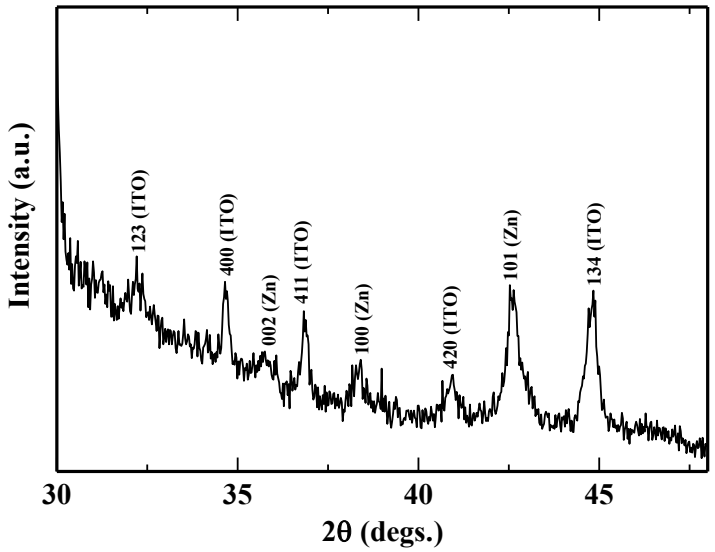

Figure s3. XRD pattern measured for the non-oxidised sample on ITO substrate. Additional Bragg reflections were identified as metallic hexagonal Zn ($P6_3/mmc$, a = 2.659 Å, c = 4.869 Å) whereas no reflections of ZnO were noticed. The sample was packed into an air-tight sample holder under Mylar® sheet in a glove box and measured immediately.